GLOBAL BIOGEOCHEMICAL CYCLES, VOL. 27, 1–13, doi:10.1002/gbc.20089, 2013

# Dynamic biogeochemical provinces in the global ocean

Gabriel Reygondeau,[1,2,3] Alan Longhurst,[4] Elodie Martinez,[2,5] Gregory Beaugrand,[6] David Antoine,[2,7] and Olivier Maury[1]

Received 18 April 2012; revised 27 June 2013; accepted 27 August 2013.

[1] In recent decades, it has been found useful to partition the pelagic environment using the concept of biogeochemical provinces, or BGCPs, within each of which it is assumed that environmental conditions are distinguishable and unique at global scale. The boundaries between provinces respond to features of physical oceanography and, ideally, should follow seasonal and interannual changes in ocean dynamics. But this ideal has not been fulfilled except for small regions of the oceans. Moreover, BGCPs have been used only as static entities having boundaries that were originally established to compute global primary production. In the present study, a new statistical methodology based on non-parametric procedures is implemented to capture the environmental characteristics within 56 BGCPs. Four main environmental parameters (bathymetry, chlorophyll *a* concentration, surface temperature, and salinity) are used to infer the spatial distribution of each BGCP over 1997–2007. The resulting dynamic partition allows us to integrate changes in the distribution of BGCPs at seasonal and interannual timescales, and so introduces the possibility of detecting spatial shifts in environmental conditions.

**Citation:** Reygondeau, G., A. Longhurst, E. Martinez, G. Beaugrand, D. Antoine, and O. Maury (2013), Dynamic biogeochemical provinces in the global ocean, *Global Biogeochem. Cycles*, *27*, doi:10.1002/gbc.20089.

## 1. Introduction

[2] The ecological geography of the oceans is not as well developed as that of the continents, but may be approached in the same manner. It is a matter of simple observation that terrestrial ecosystems may be categorized as a small number of characteristic vegetation types, or biomes, each associated with a characteristic range of environmental factors (i.e., environmental envelope): e.g., boreal coniferous forest, dry savannah, tropical deciduous forest, and arctic/alpine tundra. A simple scatterplot of mean annual precipitation against temperature identifies unique and nonoverlapping areas that represent the characteristic physiological constraints of each vegetation type, and leaves vacant those areas having combinations of temperature and rainfall that are lethal for plants [*Whittaker*, 1975]. The more advanced terrestrial mapping is capable of reproducing very faithfully the observed equilibrium global distribution of 16 vegetation types or biomes [*Haxeltine and Prentice*, 1996].

[3] A comparable approach developed lately for the oceans, because of the greater difficulty in describing the distribution of marine species and investigating their characteristic ecology. It is also widely recognized that the principal difficulty of partitioning the ocean is the dynamic movement of surface water masses and locations of surface features in response to atmospheric forcing. *Ducklow and Harris* [1993] traced the progressive evolution of an ecological partition of the upper ocean that was much influenced by the availability of the whole-ocean chlorophyll imagery from the CZCS (Coastal Zone Color Scanner, 1978–1986) sensor [*Hovis et al*., 1980] and by the requirement to plan the Joint Global Ocean Flux Study [*Scientific Committee on Oceanic Research*, 1990].

[4] In the 1980s, Margalef's analysis of the influence of turbulence and nutrients on the typology of the phytoplankton was much on everyone's mind [*Cullen et al*., 2002]. The analysis by *Platt et al*. [1991] of the seasonal/regional surface chlorophyll *a* concentration ([Chl]) from CZCS data, together with archived chlorophyll profiles and photosynthesis/irradiance measurements, led to suggest that a partition of the ocean into "biogeochemical provinces" might be both feasible and useful. Using this approach, they offered the first basin-scale computation of the primary production of phytoplankton for the North Atlantic.

Additional supporting information may be found in the online version of this article.

[1]Institut de Recherche pour le Développement, UMR EME 212, Centre de Recherches Halieutiques Méditerranéennes et Tropicales, Sète, France.
[2]Laboratoire d'Océanographie de Villefranche, CNRS–Université Pierre et Marie Curie, Villefranche-sur-Mer, France.
[3]Centre for Ecological and Evolutionary Synthesis, Department of Biosciences, University of Oslo, Oslo, Norway.
[4]Cajarc, France.
[5]Mediterranean Institute of Oceanography, Aix-Marseille University, IRD UMR 235, CNRS/INSU UMR 7294, Marseille, France.
[6]Laboratoire d'Océanologie et de Géosciences, UMR LOG CNRS 8187, Station Marine, Centre National de la Recherche Scientifique, Université des Sciences et Technologies de Lille, Wimereux, France.
[7]Department of Imaging and Applied Physics, Remote Sensing and Satellite Research Group, Curtin University, Perth, Australia.

Corresponding author: G. Reygondeau, Institut de Recherche pour le Développement, UMR EME 212, Centre de Recherches Halieutiques Méditerranéennes et Tropicales, av. Jean Monnet, B.P. 171, FR-34203 Sète CEDEX, France. (gabriel.reygondeau@gmail.fr)


0886-6236/13/10.1002/gbc.20089

**Table 1.** Information on the Environmental Data Sets Used in the Study

| Data Set | Data | Units | Type | Source |
|---|---|---|---|---|
| Environmental data set | Sea surface temperature | °C | Monthly mean from September 1997 to December 2007 | Advanced Very High Resolution Radiometer (NOAA) |
| | Sea surface salinity | g $L^{-1}$; | Monthly climatology | World Ocean Database 2005 |
| | Chlorophyll *a* concentration | mg $m^{-3}$ | Monthly mean from September 2007 to December 2007 | SeaWIFs (NASA) |
| | Bathymetry | m | Climatology | General Bathymetric Chart of the Oceans |
| Biogeochemicalprovince | Boundary | no unit | Climatology | *Longhurst* [2007] (Figure 1a) |

[5] From this, it was a relatively natural step to perform a similar analysis at a global scale [*Longhurst*, 1995; *Sathyendranath et al*., 1995]. The seasonal cycle of primary production in the global ocean was formalized into eight conceptual models, characteristic of various regions and of the environmental parameters that influence phytoplankton growth in each [cf. *Sverdrup*, 1953; *Rosa and Laevastu*, 1960]. These eight models were defined according to (i) polar irradiance-limited production peak, (ii) nutrient-limited spring bloom, (iii) winter-spring production with nutrient limitation, (iv) small-amplitude response to trade wind seasonality, (v) large-amplitude response to monsoon reversal, and (vi–viii) various responses to topography and wind stress on continental shelves, including coastal upwelling.

[6] Monthly estimates of [Chl] and mixed layer depth were obtained from the CZCS algorithm and from the NOAA-NODC global data set on a 1° grid also informed on the surface nutrient field, the Brunt-Vaisala frequency, and the Rossby radius of internal deformation [*Longhurst*, 1995; *Sathyendranath et al*., 1995]. Phytoplankton dynamics were expressed as photic depth, algal biomass and its rate of change, and primary production rate and its loss term due to consumption and sinking [*Longhurst*, 1995]. Data from the World Ocean Atlas [cf. *Levitus*, 1982] were used to locate surface discontinuities, for instance, between permanently stratified waters at low latitudes and regions where a strong mixing takes place during winter at high latitudes.

[7] From this analysis, it was concluded that the global partition would require two levels: four primary biomes (polar, westerly wind, trade wind, and coastal) that could be subdivided, logically but subjectively, into 56 smaller biogeochemical provinces [*Longhurst*, 1995]. The primary level is considered to be the equivalent of terrestrial biomes and is designed to accommodate the major responses of phytoplankton to external forcing. For ease in computation, the boundaries of provinces were laid out on a rectangular grid.

[8] This original biogeochemical partition of the ocean has been used as a template for a variety of studies ranging from the flux of organic carbon particles to the seafloor [*Honjo et al*., 2008] to the distribution of large pelagic fish [*Corbineau et al*., 2008; *Fonteneau*, 1998; *Rouyer et al*., 2008]. Overall, these studies tend to confirm that the average spatial distribution of processes and species distribution matches the pattern of the biogeochemical provinces (BGCPs), suggesting that each province does indeed exhibit characteristic environmental conditions [*Reygondeau et al*., 2012]. Recently, *Vichi et al*. [2011] showed that each province was environmentally distinct by using global observed and modeled environmental data sets rather than only surface [Chl] data. Thus, the authors suggested that the BGCP partition appears as an optimal geographical reference to distinguish the most oceanic characteristic regions at a global scale [*Vichi et al*., 2011].

[9] However, the subjective BGCPs are only a preliminary step toward objectively located boundaries that are required for operational use of provinces in many applications. Due to the growing availability of marine observations with a global- or basin-scale coverage combined with the application of multidimensional or exploratory analyses in ecology, several novel approaches have been developed to partition the global ocean in the past decades.

[10] Recent biogeographic partitions of the ocean can be divided into two main groups [*International Ocean Colour Coordinating Group* (*IOCCG*), 2009]: unsupervised and supervised partitions, to use the standard terminology of pattern recognition. Unsupervised partition proposes a partition without any spatial assumption about the oceanic structure or the environmental type of forcing, using objective methodologies (e.g., clustering analysis, ordination) to detect and map important oceanic features (e.g., frontal structures, and change in the variability of some key parameters). Several such studies have used remote-sensing observations to test and detect areas with persistent oceanographic features in the global ocean [*Hardman-Mountford et al*., 2008] as characterized by their own dynamics [*Moore et al*., 2002; *Oliver et al*., 2004; *Oliver and Irwin*, 2008; *D'Ortenzio and D'Alcalã*, 2009].

[11] Supervised partition bases the partition on a priori knowledge of the geographical structure of the area. The main advantage of using a predefined or supervised classification in a dynamical approach is to keep a link between the general description of the oceanographic patterns and their ecological composition [*IOCCG*, 2009]. Therefore, updates of the original partition proposed by recent studies allow a more realistic refining of the original boundaries by reproducing the ocean dynamics [*Devred et al*., 2007; *Forget et al*., 2010; *Platt and Sathyendranath*, 2008; *Platt et al*., 2005].

[12] To date, no implementation of the BGCP concept has captured the influence of changing environmental conditions on the spatial distribution of the provinces at global scale, although boundaries between ecological provinces in the NW Atlantic have been observed to change at the decadal scale [*Devred et al*., 2009]. In the present study, a new supervised partition based on the Non-Parametric Probabilistic Ecological Niche Model (NPPEN) [*Beaugrand et al*., 2011] is implemented to capture characteristics of 56 BGCPs using four main environmental parameters (bathymetry, [Chl], sea surface temperature, and sea surface salinity).

Using nonparametric linkages with environmental factors inferred from the NPPEN outputs, the probability of occurrence, the average latitude, and the average area of each BGCP are computed for the Sea-viewing Wide Field-of-view Sensor (SeaWiFS) period (1997–2007) at a monthly and annual time scale. The inferred dynamic ecological provinces are presented in this study and, based on the inferred dynamic biogeography, the spatial changes of the BGCPs at seasonal and interannual time scales have been explored.

## 2. Materials and Methods

### 2.1. Data

[13] Sea surface temperature (SST), bathymetry, sea surface salinity (SSS), and [Chl] are used in the present work over the global ocean from 179.5°W to 179.5°E and from 89.5°N to 89.5°N and on a 1° × 1° grid (Table 1).

[14] We used SST because of its cardinal influence on biogeochemical systems [*Brander*, 2009]; monthly SST was extracted from the Advanced Very High Resolution Radiometer (AVHRR) data set (http://podaac.jpl.nasa.gov/PRODUCTS/) [*Holben*, 1986] for the 1997–2007 time period.

[15] Bathymetry helped principally to distinguish continental shelf (<200 m) from open ocean regions, an important distinction ecologically, recognized in the global partition of biomes by *Longhurst* [1995]. Bathymetry was downloaded from the General Bathymetric Chart of the Oceans [*Smith and Sandwell*, 1997].

[16] SSS also enables the discrimination of systems such as subtropical oceanic gyres from regions influenced by river inflow [*Sarmiento and Gruber*, 2006]. Because no comprehensive and validated global time series of SSS was currently available, monthly and annual climatologies were taken from the World Ocean Atlas 2005 [*Antonov et al*., 2006].

[17] [Chl] was used as a proxy of phytoplankton abundance at a global scale [*McClain*, 2009; *Longhurst*, 1995]. We used the standard SeaWiFS 2009.1 reprocessing data set made available on a monthly grid from September 1997 to December 2007 from NASA at http://oceandata.sci.gsfc.nasa.gov/ [*McClain et al*., 2004]. The data set is averaged at a monthly time step from September 1997 to December 2007 and at a spatial resolution of 1° of latitude and longitude.

### 2.2. Methods

[18] Based on the knowledge of the supervised BGCPs established by *Longhurst* [2007] (Table 2 and Figure 1) and the four environmental parameters, we set up a procedure to examine how distributions of BGCPs fluctuate in space and time at seasonal and interannual scales. The different steps are summarized in Figures 1 and 2.

#### 2.2.1. Step 1: Identification of the Environmental Conditions Within Each Reference BGCP

[19] To allocate appropriate values for the four parameters discussed above to each biogeochemical province, the spatial coordinates of each BGCP were first retrieved from the latest version of the partition of *Longhurst* [2007] (Figure 1). We subsequently attributed to each geographical cell a value for SST and [Chl] for each month of the period ranging from September 1997 to December 2007 (124 months), a value of SSS for each corresponding month (12 months) and a single value for bathymetry. We thus obtained our 56 reference matrices (one for each province) named $\mathbf{X}_{n,p}$ ($n = 124$ months multiplied the number of geographical cells, $p = 4$ environmental variables).

**Table 2.** Information on the 56 Biogeochemical Provinces Identified by *Longhurst* [2007][a]

| Province Name | Code | Biome | Ocean |
|---|---|---|---|
| Southwest Atlantic shelves | FKLD | Coastal | Atlantic |
| Brazilian current coast | BRAZ | Coastal | Atlantic |
| Benguela current coast | BENG | Coastal | Atlantic |
| Guinea current coast | GUIN | Coastal | Atlantic |
| Canary current coast | CNRY | Coastal | Atlantic |
| Guianas coast | GUIA | Coastal | Atlantic |
| Northeast Atlantic shelves | NECS | Coastal | Atlantic |
| Northwest Atlantic shelves | NWCS | Coastal | Atlantic |
| Atlantic Arctic | ARCT | Polar | Atlantic |
| Atlantic sub-Arctic | SARC | Polar | Atlantic |
| South Atlantic gyral | SATL | Trade wind | Atlantic |
| Eastern tropical Atlantic | ETRA | Trade wind | Atlantic |
| Western tropical Atlantic | WTRA | Trade wind | Atlantic |
| Caribbean | CARB | Trade wind | Atlantic |
| North Atlantic tropical gyral | NATR | Trade wind | Atlantic |
| Northeast Atlantic subtropical gyral | NAST E | Westerly | Atlantic |
| Mediterranean Sea | MEDI | Westerly | Atlantic |
| Northwest Atlantic subtropical gyral | NAST W | Westerly | Atlantic |
| Gulf Stream | GFST | Westerly | Atlantic |
| North Atlantic Drift | NADR | Westerly | Atlantic |
| Humboldt current coast | HUMB | Coastal | Pacific |
| East Australian coast | AUSE | Coastal | Pacific |
| Sunda-Arafura shelves | SUND | Coastal | Pacific |
| China Sea | CHIN | Coastal | Pacific |
| Central American coast | CAMR | Coastal | Pacific |
| Alaska coastal downwelling | ALSK | Coastal | Pacific |
| New Zealand coast | NEWZ | Coastal | Pacific |
| Coastal Californian current | CCAL | Coastal | Pacific |
| North Pacific epicontinental sea | BERS | Polar | Pacific |
| Archipelagic deep basins | ARCH | Trade wind | Pacific |
| Pacific equatorial divergence | PEQD | Trade wind | Pacific |
| North Pacific equatorial counter current | PNEC | Trade wind | Pacific |
| North Pacific Tropical gyre | NPTG | Trade wind | Pacific |
| California current | C(O)CAL | Trade wind | Pacific |
| South Pacific gyre | SPSG | Trade wind | Pacific |
| Western Pacific warm pool | WARM | Trade wind | Pacific |
| Tasman Sea | TASM | Westerly | Pacific |
| Kuroshio current | KURO | Westerly | Pacific |
| Eastern Pacific subarctic gyres | PSAE | Westerly | Pacific |
| Western Pacific subarctic gyres | PSAW | Westerly | Pacific |
| North Pacific polar front | NPPF | Westerly | Pacific |
| Northwest Pacific subtropical | NPSW | Westerly | Pacific |
| Northeast Pacific subtropical | NPSE | Westerly | Pacific |
| Eastern India coast | EAFR | Coastal | Indian |
| Western Australian and Indonesian coast | AUSW | Coastal | Indian |
| Eastern India coast | IND E | Coastal | Indian |
| Red Sea, Arabian Gulf | REDS | Coastal | Indian |
| Western India coast | IND W | Coastal | Indian |
| Indian South subtropical gyre | ISSG | Trade wind | Indian |
| Indian monsoon gyre | MONS | Trade wind | Indian |
| Northwest Arabian Sea upwelling | ARAB | Westerly | Indian |
| South subtropical convergence | SSTC | Westerly | Antarctic |
| Subantarctic water ring | SANT | Westerly | Antarctic |
| Antarctic | ANTA | Polar | Antarctic |
| Austral polar | APLR | Polar | Antarctic |
| Boreal polar | BPRL | Polar | Arctic |

[a]Name, abbreviation, biome, and ocean of each province are listed.

#### 2.2.2. Step 2: Characterization of the Environmental Envelope of Each BGCP

[20] The method applied to define the environmental envelope of each BGCP was based on the Non-Parametric

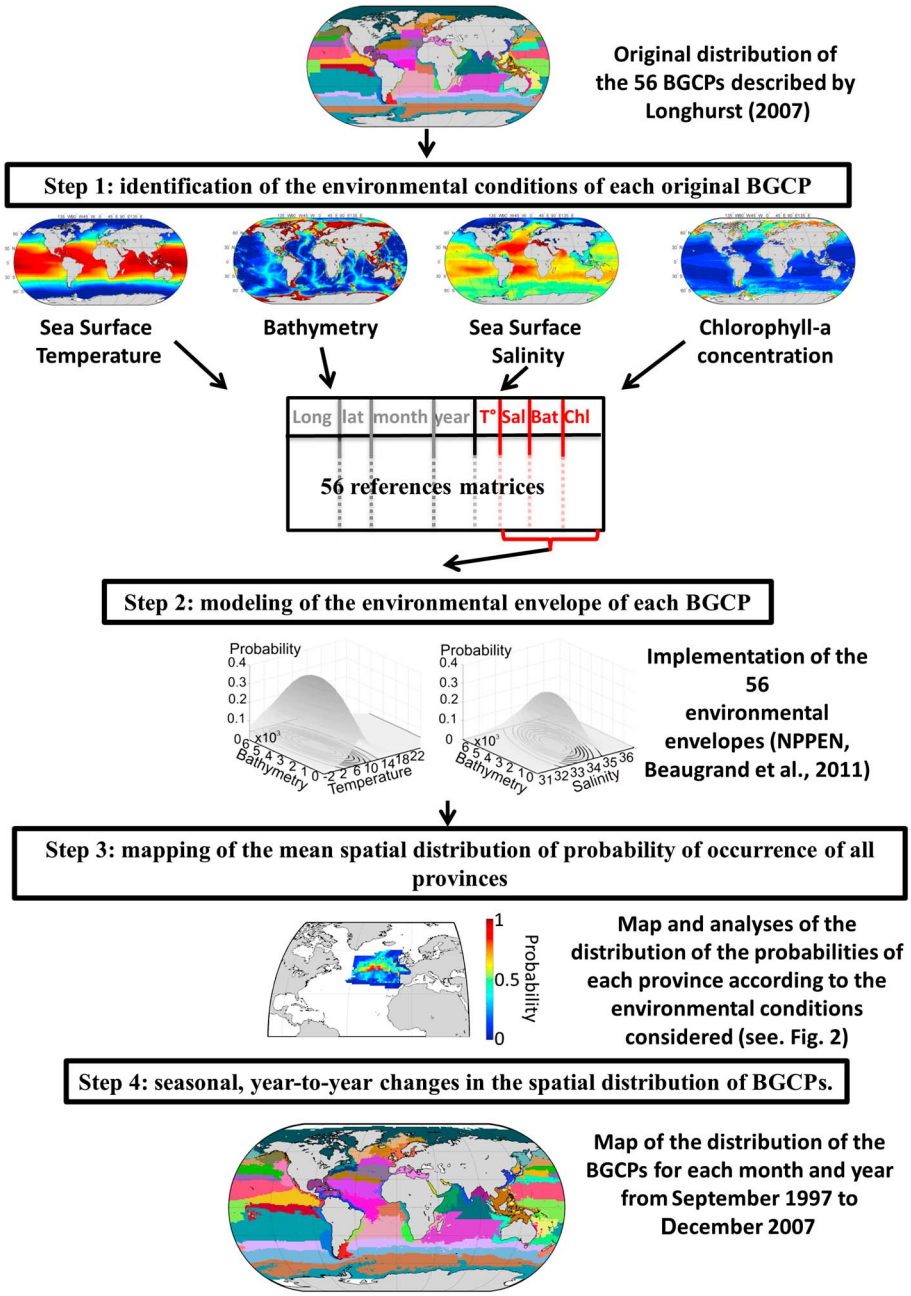


**Figure 1.** Schematic representation of the numerical procedures used in this study (see section 2 for details). Specific details about step 3 can be retrieved from Figure 2.

Probabilistic Ecological Niche Model (NPPEN) [*Beaugrand et al.*, 2011]. A prerequisite for the application of the method consisted in identifying and removing any replicates in the reference matrices that could bias the NPPEN method [*Beaugrand et al.*, 2011; *Lenoir et al.*, 2011; *Goberville et al.*, 2011; *Reygondeau and Beaugrand*, 2011]. To do so, we characterized the observation density as a function of the four environmental parameters considered (SST, [Chl], SSS, and bathymetry) for each reference matrix $\mathbf{X}_{n,\mathrm{p}}$. Thus, a four-dimension matrix was built with each dimension corresponding to one environmental parameter. Each dimension was discretized according to a fixed environmental range and step: Range of SST is considered from −2°C to 32°C and subdivided every 0.5°; SSS was ranging from 0 to 40 and subdivided every 0.2; ranges of bathymetry were fixed between 0 and 8000 m with intervals of 100 m and ranges of [Chl] were fixed from $\log_{10}$ 0.001 to 5.0 mg $m^{-3}$ and subdivided every 0.1 [*Campbell*, 1995]. To compute the observation density, the number of observation in the reference matrix was calculated for each four-dimensional interval. Only four-dimensional intervals with at least five observations were retained and then averaged.

[21] We tested the sensitivity of the simplification procedure of the NPPEN method using several thresholds

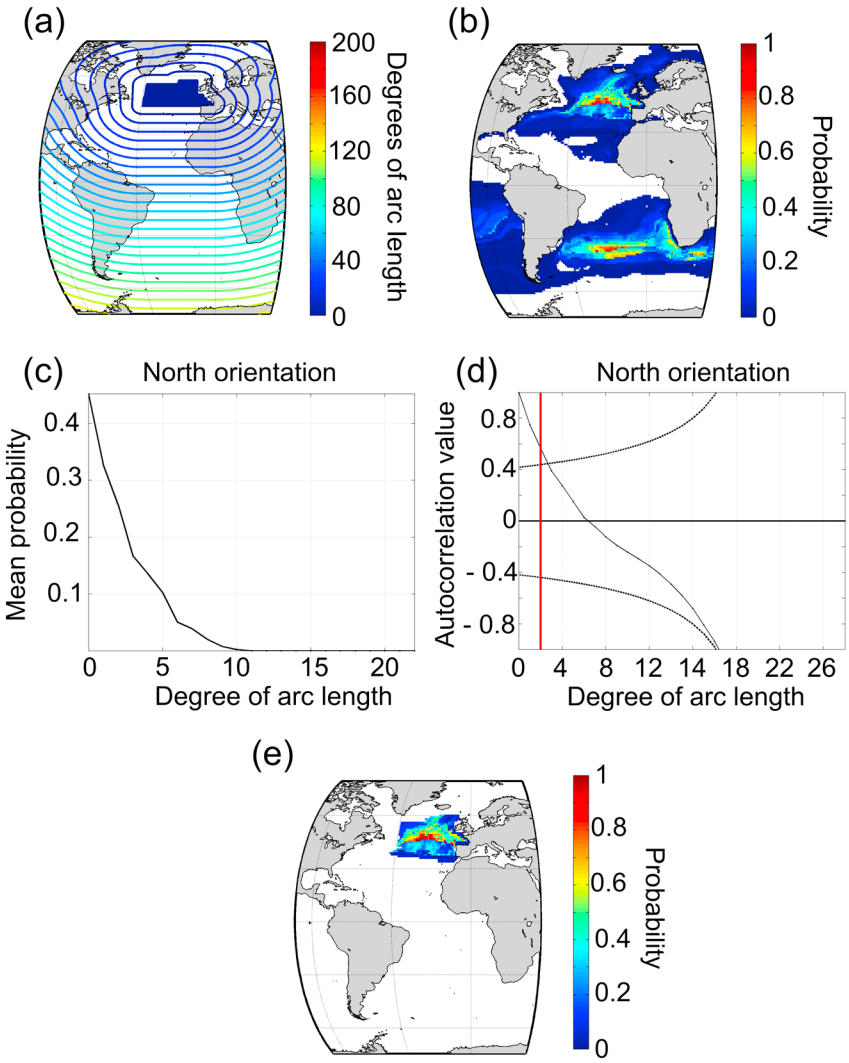


**Figure 2.** (a) Distance (degree of arc length) from the boundary of the province NADR. (b) Map of the raw probability of the province NADR. (c) Mean probability of the province NADR per degree of arc length for the north orientation. (d) Simplified Moran index for each step of degree of arc length using the probability of the NADR in the north orientation. (e) Map of the spatial distribution of the resulting probability of the province NADR.

for the discretization of each environmental parameter (Figure S1 in the supporting information). The required number of observations was also tested. We found very similar outcomes, except when choosing one observation and/or a too wide environmental discretization. Finally, we selected the minimum number of observations and the thresholds used for the environmental discretization as a compromise between a too elevated variance in the reference matrix (especially when only one value or a too wide discretization was chosen) and too many missing data in the matrix (when the minimum number of observations was too high).

[22] Each of the 56 simplified reference matrices (i.e., $\mathbf{X}\mathrm{sim}_{n,p}$) were then modeled by the NPPEN. This statistical method tests the probability that random observation $x$ characterized by four environmental parameters belongs to a simplified reference matrix, $\mathbf{X}\mathrm{sim}_{n,p}$. The NPPEN uses the generalized Mahalanobis distance [*Mahalanobis*, 1936] that enables the correlation between variables to be taken into account [*Ibañez*, 1981]:

$$D^2_{x,\mathbf{X}} = (x - \overline{E})' R^{-1} (x - \overline{E}), \tag{1}$$

with $x$ the vector of length $p$ representing the values of the four environmental parameters to be tested, $R_{p,p}$ the correlation matrix of the simplified reference matrix $\mathbf{X}\mathrm{sim}_{n,p}$, and $E$ the average environmental parameter inferred from $\mathbf{X}\mathrm{sim}_{n,p}$. The procedure is based on a simplified version of the multiple response permutation procedure [*Mielke et al.*, 1981], which was described in *Beaugrand and Helaouët* [2008] and in *Lenoir et al.* [2011]. The calculation of the Mahalanobis generalized distance and its probability was repeated $m$ times, with $m$ the number of observations $x$ to be tested. The NPPEN produces the probability to find the environmental envelope of a province as a function of our four parameters (SST, SSS, [Chl], and bathymetry). Further

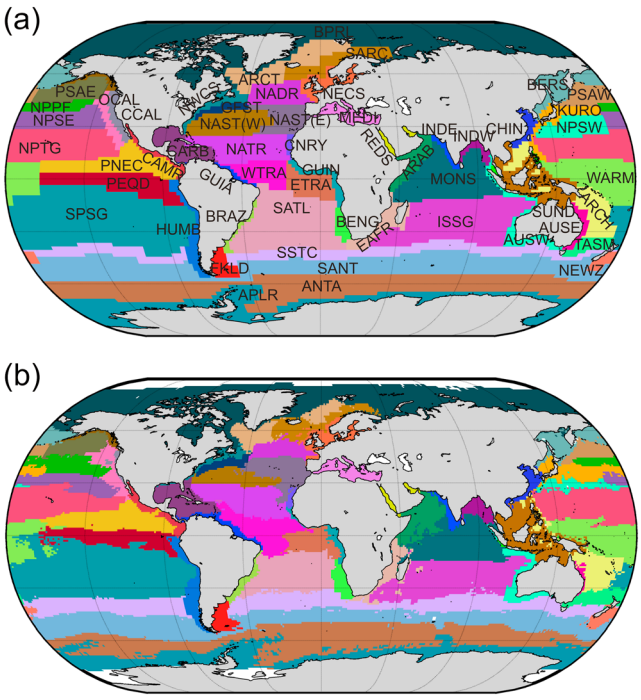


**Figure 3.** Biogeography of the global ocean (i.e., biogeochemical provinces) proposed by (a) *Longhurst* [2007] and (b) calculated in this study for the average period from January 1998 to December 2007.

information on the rationale and the mathematics of NPPEN can be found in *Beaugrand et al*. [2011].

#### 2.2.3. Step 3: Mean Spatial Distribution of Probability of Occurrence to BGCPs

[23] Considering a reference BGCP (the NADR province for instance in Figure 2a), we obtained from step 2 a map of the probability to belong to this reference province (Figure 2b). As shown on Figure 2b, a high probability to belong to this reference province can also appear in similar oceanic environment, i.e., in opposite hemisphere or different oceanic basins. As our focus is based on the BGCPs of *Longhurst* [2007], we retained only those geographical cells that were both environmentally and spatially autocorrelated to this original division. To remove the geographical cells with high environmental similarity but located in other basins or/and in the other hemisphere, we implemented a procedure that is based on Moran's *I* index [*Legendre and Legendre*, 1998]. We however simplified the procedure by fixing all spatial weights to 1. All steps of the procedure are summarized on Figure 2.

[24] First, we calculated the barycenter of each BGCP. Then, we calculated the distance between the barycenter of each province and all other geographical cells, considering the geographical coordinates and the ellipsoid of the Earth using the Matlab mapping toolbox © in degree of arc length (Figure 2a). The angle between each geographical cell and the barycenter of the province was calculated. Then, each probability (Figure 2b) was attributed to a given direction (Figure 2c). Eight directions were possible: N, NE, E, SE, S, SW, W, and NW. Finally in each direction, we calculated the simplified Moran's *I* index. We only retained geographical cells that were significantly correlated with the barycenter of the province (Figure 2d) using a threshold of probability of the autocorrelation of 0.05 [*Legendre and Legendre*, 1998; *Dorman et al*., 2007]. All geographical cells of the province as originally defined by *Longhurst* [2007] were retained (Figure 2e).

#### 2.2.4. Step 4: Seasonal and Interannual Changes in the Spatial Distribution of BGCPs

[25] To map the spatial variability of the BGCPs, environmental conditions were time averaged for each geographical cell and for the following time periods: (1) annual mean from January 1998 to 2007 (Figure 3), (2) monthly mean from January 1998 to December 2007 (Figure 4 and Animation S1), and (3) El Niño (from September 1997 to April 1998) and La Niña (June 1998 to March 2001) events (Figures 7a and 7b). We also considered (4) the monthly time series from September 1997 to December 2007. The spatial distribution of the 56 BGCPs was computed and mapped according to these four time conditions. Then, for each geographic cell, only the province with the maximal probability was retained, thereby providing a general distribution of the 56 BGCPs. However, for a given geographic cell and at a given time, the values of the four environmental parameters were needed to retrieve the probability to belong to BGCPs. If at least one parameter was missing (e.g., due to cloud density or ice cover), the geographical cell was not considered by our procedure and no probability values were attributed.

### 2.3. Definition and Temporal Survey of the Spatial Characteristics of the BGCPs

[26] To characterize the spatial variability of each BGCP, three estimators were computed: mean latitude and longitude of the centroid, and the total area of the BGCPs. These three parameters were calculated for BGCPs derived from environmental conditions yearly and monthly averaged (see 1 and 2 in the previous paragraph). The mean latitude, longitude, and area of each BGCP were calculated using the *geographic statistic* of the Matlab® mapping toolbox. To quantify the seasonal spatial variation of each BGCP, boxplots of the mean latitude and longitude and the coefficient of variation of the area are drawn in Figure 5.

[27] To evaluate how the probabilities of a geographical cell to belong to BGCPs can vary in time and overlap with adjacent provinces, an index of stability was computed over the probability of each of the BGCPs using the monthly time series from January 1998 to December 2007 (Figure 6). We used the Simpson dominance index [*Beaugrand and Edwards*, 2001]. The higher the index, the more stable the geographical cell was in time. Therefore, low values of the index revealed areas of high spatiotemporal changes in the environmental conditions and conversely.

### 2.4. BGCPs Variability Under Normal, La Niña, and El Niño Conditions

[28] Here we examined the influence of El Niño–Southern Oscillation (ENSO) events on the spatial distribution of the BGCPs. The influence of interannual physical variability on oceanic biogeography was investigated by comparing the spatial distribution of provinces during El Niño and La Niña events and normal conditions. To do this, time series of the extratropical Northern Oscillation Index (NOI) was used to identify the different climatic conditions from September 1997 to December 2007. NOI was selected because it well reflects interannual changes in the climatic

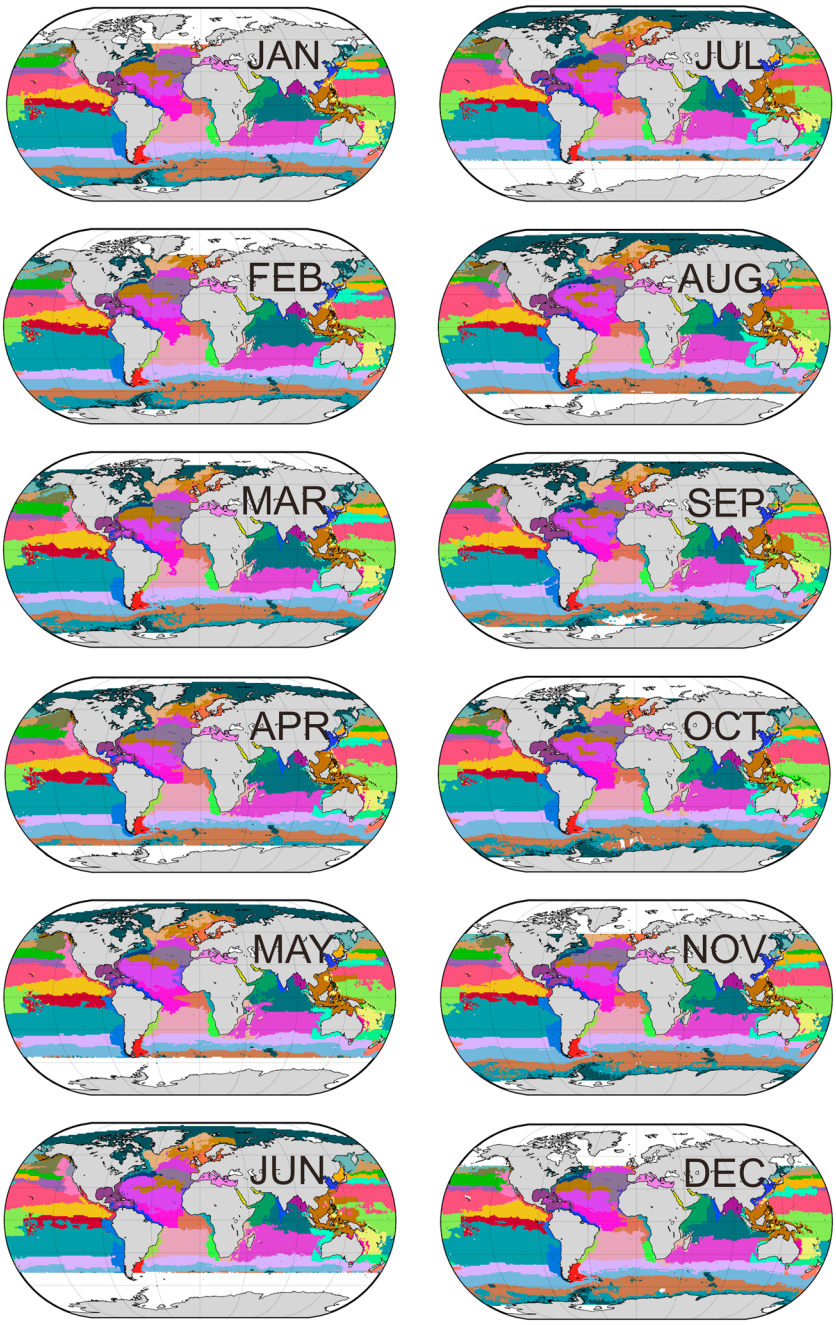


**Figure 4.** Monthly climatology of the spatial distribution of the biogeochemical provinces computed for the period from September 1997 to December 2007.

regime of both equatorial and extratropical areas of the Pacific Ocean [*Schwing et al*., 2002].

[29] Months were allocated to El Niño events if the NOI was below an empirical threshold of −1.25 (31 months), to La Niña events above a threshold of +1.25 (40 months), and to normal conditions when the value was between these two thresholds (53 months). The thresholds were fixed by confronting the index variation to the well-identified 1997/1998 El Niño and 1998/1999 La Niña events. The spatial variations of BGCPs undergone during the strongest El Niño (September 1997 to April 1998) and La Niña events (June 1998 to March 2001) over 1997–2007 were mapped on Figures 7a and 7b, respectively. Furthermore, comparisons between El Niño, La Niña and normal conditions that have occurred over the whole time period (1997–2007) were performed using a *t* test on the probability of occurrence. The statistical procedure was performed by comparing for each geographical cell the probabilities of occurrence between two different climatic events (with at least five observations per climatic events and geographical cell). Then, *p* values showing significant differences between the two tested climatic events ($p$ value $\leq 0.05$) were

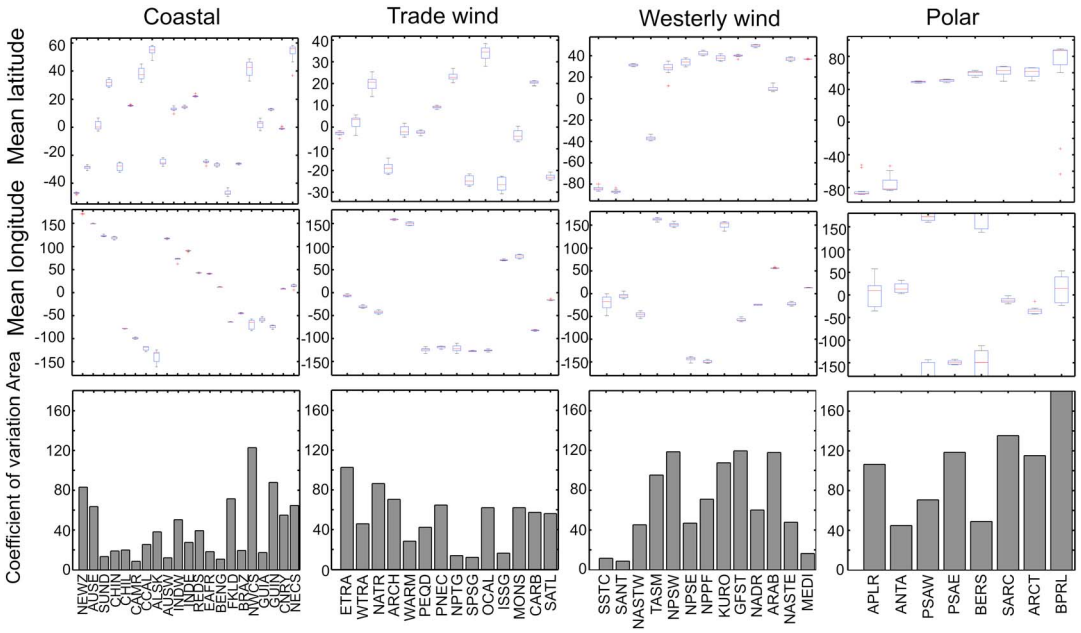


**Figure 5.** Boxplot of the seasonal variation of the (top row) mean latitude (decimal degree), (middle row) mean longitude (decimal degree), and (bottom row) coefficient of variation of the area (km$^2$) of the 56 biogeochemical provinces according to the monthly climatology (Figure 4).

mapped. We performed three comparisons: (i) El Niño versus normal conditions (Figure 7c), (ii) La Niña versus normal conditions (Figure 7d), and (iii) El Niño versus La Niña (Figure 7e).

## 3. Results

### 3.1. A Dynamic Revision of the Longhurst Partition of the Global Ocean

[30] The spatial distribution of the 56 BGCPs that we obtained from January 1998 to December 2007 (Figure 3b) was close to the partition proposed by *Longhurst* [2007] (Figure 3a). This result was expected as Longhurst BGCPs served as a baseline to construct ours.

[31] However, our technique enabled here a better delineation of the boundaries of the provinces according to environmental gradients and oceanographic features. Indeed, spatial distributions of some BGCPs in the continental biome (BRAZ, CAMR, CCAL, INDE, SUND, NWCS, or NECS) showed a better demarcation of the bathymetric gradient that divided open sea and continental shelf areas around 200 m [*Longhurst*, 1995]. An improved identification of some specific oceanographic features also appeared such as in equatorial upwelling regions (ETRA, PEQD, and ARAB), subtropical gyre systems (NAST, ISSG, and NPTG), and well-known currents such as the Algulhas (EAFR), the Gulf Stream (GFST), or the Kuroshio (KURO) currents [*Tomczak and Godfrey*, 2003]. In the polar and westerly wind biomes, variations in the spatial distribution of some BGCPs (SSTC, ANTA, SANT, and BPRL) better identified the latitudinal temperature-primary productivity than in the original BGCPs, because our results are driven by environmental parameters.

### 3.2. Seasonal Changes in the Spatial Distribution of BGCPs

[32] The main seasonal spatial movement of the 56 BGCPs was related to the meridional seasonal variability of the incoming solar irradiance in extratropical regions, combined with seasonal changes in stratification (Figure 4 and Animation S1). The mean latitude of BGCPs moved poleward during boreal summer and spring, and equatorward during winter and autumn of their respective

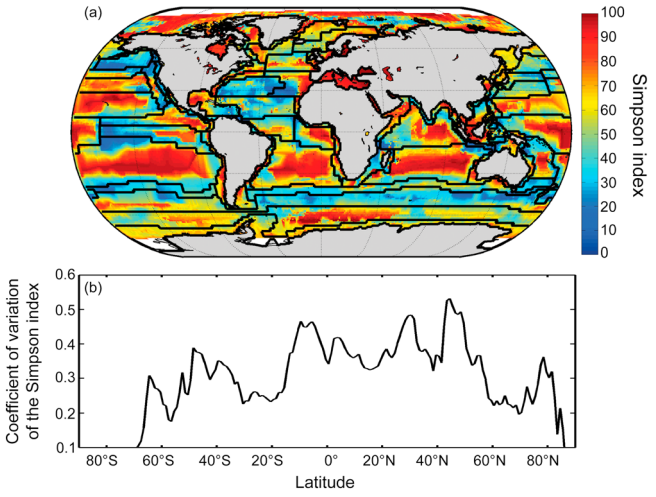


**Figure 6.** Map of the seasonal overlap between the 56 BGCPs computed using the Simpson index. The higher the index, the more stable the pixel is in time. Therefore, low values of the index reveal variable regions in term of their province composition and belonging.

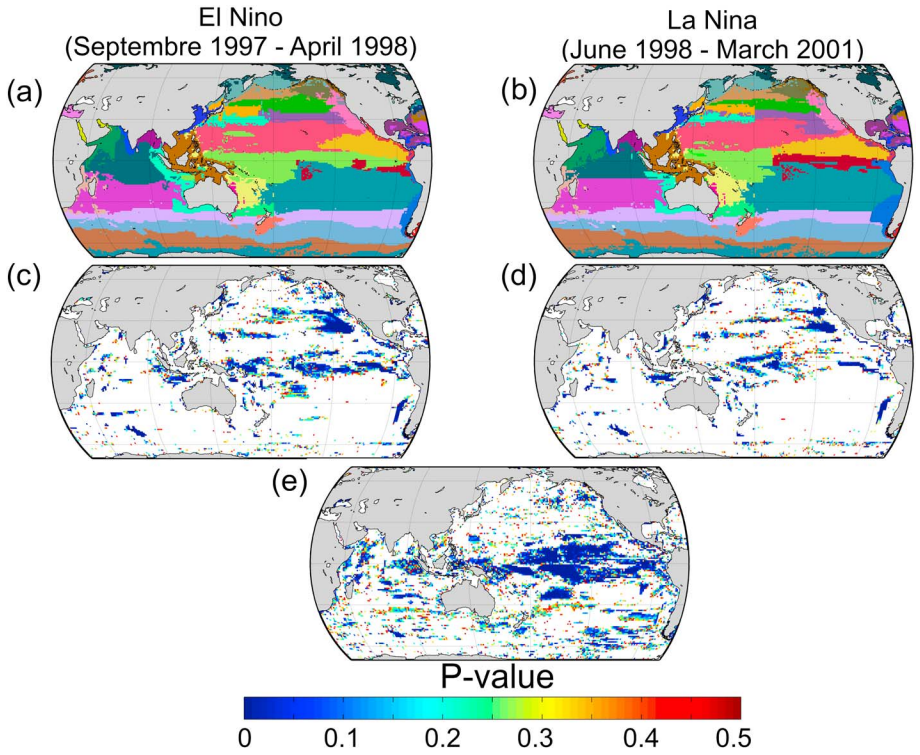


**Figure 7.** (a) Biogeography of the global ocean for the 1997/1998 El Niño event (September 1997 to April 1998). (b) Biogeography of the global ocean for 1998/2001 La Niña event (July 1998 to March 2001). (c) Map of the significant change ($p$ value $\leq 0.05$) in the probability of occurrence between El Niño months and normal conditions. (d) Map of the significant change ($p$ value $\leq 0.05$) in the probability of occurrence between La Niña months and normal conditions. (e) Map of the significant change (p-value $\leq 0.05$) in the probability of occurrence between El Niño months and La Niña months. The extratropical Northern Oscillation Index was used to detect the El Niño, La Niña, and normal conditions.

hemispheres. This latitudinal seasonal displacement revealed that provinces with the highest seasonal movements were located north of 30° in latitude and mostly belonged to the westerlies wind and polar biomes (Figure 4 and Animation S1). The latitudinal displacements of the BGCPs ranged between 3° for tropical provinces and up to 18° in polar provinces (Figure 5, top row).

[33] Longitudinal seasonal changes in the spatial distribution reached up to 27° of longitude (Figure 5, middle row). This spatial change can firstly be attributed to a lag time between the periods of high biological productivity (bloom period). Then, the longitudinal movement of the provinces can be attributed for instance to seasonal displacements of surface water masses as for the jet streams (Gulf Stream and Kuroshio) or to atmospheric events (monsoon affecting the whole Indian Ocean) (Figure 4 and Animation S1).

[34] Both longitudinal and latitudinal movements induced seasonal variations in BGCP areas (Figure 5, bottom row). Tropical provinces exhibited a summer expansion of their areas when adjacent westerlies provinces moved poleward. The westerlies provinces expanded between middle of spring to end of summer (of their respective hemisphere) due to highest latitudinal shift of their northern boundaries than their southern boundaries (Figures 4 and 6 and Animation S1). Simultaneously, areas of polar provinces decreased, especially in the Northern Hemisphere. Then, during autumn and winter, areas of polar provinces expanded while they contracted in westerlies provinces. However, the lack of remote-sensing observations due to high cloud coverage during wintertime can limit the detection of the mean latitude and longitude of the centroid and the total area of the BGCPs in polar and high latitude westerlies provinces, and results need to be considered with caution.

[35] Finally, a Simpson index was used to examine simultaneously the time variability and the overlap between the probabilities of occurrence of the 56 BGCPs (Figure 6). The Southern Ocean exhibited an index value from 50 to 70% between the Antarctic coasts and the polar front (60°S). This high value reflected a low seasonal variability and a low overlap between the probabilities of occurrence of the regional BGCPs. This can be mainly attributed to the lack of remote-sensing observations during more than half of the year and consequently to a time variability not accurately represented. Offshore the Queen Maud Land, the most stable area of the Southern Ocean appeared (Figure 6 and Animation S1). The area between the polar front and the subtropical front exhibited a low index (from 0 to 30%), showing an important overlap between the probabilities of occurrence of the BGCPs and a high seasonality (Animation S1).

[36] The Arctic Ocean also exhibited high index values in high latitudes that can be attributed to a lack of observation and ice cover. Variations of the index occurred in the Barents, Laptev, and Kara Seas with an index value between 0 and 40% (Figure 6). Furthermore, all the well-known frontal dynamical areas were detected in each of the ocean basins and exhibited a Simpson index value smaller than 50% such as along the oceanic polar front, along the subtropical convergence area of the Atlantic Ocean, along the northern and southern polar fronts, the Sitka Front in the Pacific Ocean, and in the subtropical convergence area of the Indian Ocean, located between the provinces MONS and ISSG (Figure 4 and Animation S1).

[37] Low index value (e.g., highly variable areas) was detected in the trade wind biomes as in the convergence zone between the warm pool (WARM) and the eastern equatorial provinces, along the frontal structure between the Humboldt upwelling and the oceanic area, the Mozambique channel, the cyclonic front of the Zanzibar current, the Sunda-Arafura Sea and the Agulhas Current in the Indian Ocean, the Atlantic Counter Current, and the oceanic polar front (Figure 6). Stable areas (high index value) were mainly located in the core of the subtropical gyres, along the continental shelves and in the Arabian and Mediterranean Seas (Figure 6). The North East Atlantic Subtropical regions (i.e., NASTE) exhibit a low index value compared to other subtropical gyres and hence is more comparable to a boundary current region of the ocean.

### 3.3. BGCP Variability During El Niño and La Niña Events

[38] The effect of climatic events on our partition of the global ocean was investigated by comparing the probability of occurrence of each BGCP during El Niño and La Niña events and normal conditions. El Niño 1997/1998 and La Niña 1998/2001 were mapped to visualize the changes in the spatial distribution of the BGCPs occurring during these specific events (Figures 7a and 7b). Then, the probability of occurrence between the different events has been investigated over 1997–2007 (Figures 7c and 7d).

[39] During El Niño events (Figures 7a and 7c), the Pacific Ocean was the basin most affected with an eastward extended warm pool (WARM), while areas of the eastern equatorial Pacific provinces (PNEC and PEQD) and the Pacific archipelagic deep basin provinces (ARCH) were much reduced (Table S1). In addition, the adjacent gyre provinces (SPSG and NPTG) expanded their boundaries to the equator, thus decreasing the surface of the PNEC and PEQD provinces as well as those of the upwelling provinces (e.g., CCAL or HUMB). The Indonesian continental shelf was affected by El Niño events by a change in its probability of occurrence due to the incursion of the WARM province into the Arafura Sea (Figure 7c). In the eastern Indian Ocean, the warm provinces MONS and AUSW increased their area southward and northward, respectively, whereas the Arabian Sea and the Indian Ocean subtropical gyre provinces (respectively in the northwest and south of the Indian Ocean) contracted.

[40] La Niña events mainly affected the Pacific Ocean with an expansion of the areas in equatorial provinces (PNEC and PEQD) as well as in the Humboldt and the archipelagic ecosystems provinces (HUMB and ARCH) and a reduction of the area of their adjacent provinces (SPSG, WARM, NPTG, and CAMR) (Figure 7b and Table S1). The subpolar Pacific and Northern westerlies provinces also exhibited important changes in their probability of occurrence, thus modifying the average spatial distribution of the boundaries in the basin (Figure 7d). The Kuroshio ecosystem province area increased eastward (Table S1), displacing the North Pacific Subtropical Province (NPSE) to the south. In contrast, the biogeography in the Indian and Atlantic Oceans changed slightly to the La Niña events. Meanwhile, polar and westerly wind biomes of the Southern Ocean showed a wide latitudinal change in their spatial distribution leading to the contraction of the polar provinces.

## 4. Discussion

[41] Over the last decades, several types of partitions of the oceanic domain have been proposed, each attempting to identify unique marine ecological units (biotopes and biocenoses) such as Large Marine Ecosystems [*Sherman*, 2005] or Marine Ecoregions of the World [*Spalding et al*., 2007]. The partition into 56 biogeochemical provinces proposed by *Longhurst* [2007] has been widely used as a geographical reference for ecological studies and provides an ecological/environmental partition that encompasses both continental shelves and open oceans [*Vichi et al*., 2011].

[42] However, the static boundaries of the BGCP partition have been criticized because they do not respond to the temporal dynamics of the ocean over longer than annual time periods [*Pauly et al*., 2000]. In its original form, each BGCP was described as an ecological partition of the global ocean, based on definable and observable boundaries that encompassed regions each having characteristic cycles of primary production that could be accommodated within just four types of biomes. The results presented here are highly dependent on the reliability of the division proposed by *Longhurst* [2007] as any other supervised oceanic partitions. However, by characterizing the environmental envelope of each BGCP, our procedure (Figure 1) enabled us to quantify the heterogeneity of each province according to a selected data set at a global scale and allowed the static partition to become more dynamic in space and time (Figures 3, 4, and 7).

[43] Our procedure captured the seasonal changes in the locations of the provinces (Figure 4 and Animation S1) already reported in literature [*Devred et al*., 2007; *IOCCG*, 2009; *Vantrepotte and Mélin*, 2010], with a stronger seasonality in high latitudes (Figure 5). Provinces belonging to trade wind biomes (<30° of latitude), especially in the subtropical gyres, extended during summer and contracted during winter, as shown in previous works [*Irwin and Oliver*, 2009; *Polovina et al*., 2008]. Provinces belonging to the westerly wind biomes moved poleward during summer and equatorward during winter in phase with SST seasonal variability. Longitudinal variation caused by climatic events (e.g., monsoon events), tropical upwelling, or change in the surface currents was also captured by the methodology. Nonetheless, due to the size of

the provinces and the rough resolution of the environmental data sets (i.e., 1° longitudes × 1° latitudes), seasonal mesoscale features such as eddies or current meanders were not detected by the present procedure [*Devred et al*., 2007; *Oliver and Irwin*, 2008].

[44] The seasonal movement of the 56 BGCPs was also summarized using the Simpson index for the period from September 1997 to December 2007 (Figure 6). The index helped to illustrate the biogeographical stability of each geographical cell and to identify the two base components of BGCPs. Regions with low Simpson index correspond to highly variable environmental areas such as seasonal extent of BGCPs. Regions with high values of the index are attributed to the same environmental envelope throughout time and are here defined as BGCP's core areas. Seasonal extents of the BGCPs are of major importance for global and regional ecological and biogeochemical processes as they provide a bridge for the exchange of particulate and dissolved matter between provinces. According to the latitudinal coefficient of variation of the index (Figure 6b), BGCPs with a higher proportion of seasonal extent are mainly retrieved in frontal structure areas (SANT, SSTC, and NPTG) or in province defined by specific currents (GFST and KURO). Conversely, areas characterized by a higher proportion of core regions are mainly located in subtropical and polar gyres at the exception of the North Atlantic subtropical province as *Vichi et al*. [2011] already observed. These regions represent areas where climate fluctuations are not expected to alter the characteristic environmental conditions of the BGCP.

[45] Previous studies have shown significant changes of environmental conditions during ENSO events [*Cobb et al*., 2003; *Tomczak and Godfrey*, 2003] that are assumed to reorganize the ecological partition of the Pacific and Indian Oceans [*Longhurst*, 2007]. Here we investigated the effects of El Niño (Figures 7a and 7c) and La Niña (Figures 7b and 7d) events on our BGCP distribution. Our results reveal that changes in environmental conditions drive spatial reorganization of the BGCPs during ENSO events at a basin scale. Due to the important time lag in the atmospheric teleconnection allowing ENSO events to affect the global ocean, the use of the present methodology did not enable us to detect changes in other oceans, which would be attributable to ENSO events.

[46] During El Niño events, the observed expansion of the trade wind provinces (WARM, MONS, ISSG, NPTG, and SPSG) may be attributed to the eastward inflow of warm waters in the tropical Pacific [*Cobb et al*., 2003; *Meyers et al*., 2007]. This eastward advection is mainly driven by a weakening of the easterlies along the equatorial belt and induces shallower thermocline in the west and deeper thermocline in the east. These changes in the thermocline depth influence the input of nutrient to the surface and thus productivity [*Messié and Chavez*, 2012; *Radenac et al*., 2012]. The opposite patterns are observed during La Niña events. These modifications of the environmental conditions are well captured by the present methodology using only two parameters informed in time (i.e., monthly SST and monthly [Chl]) that introduce a spatial modification of BGCP distribution during ENSO events. A future task to better investigate the effect of ENSO on the global distribution of BGCPs would be to introduce new environmental parameters as winds and/or sea level anomaly (as an indicator of the thermocline depth) derived from remote sensing. Based on this adjustment of the method, we should be able to test the sensitivity of the different parameters in the modeling of BGCPs under ENSO conditions.

[47] Environmental envelopes of each BGCP are inferred from reference matrix (see step 2 in section 2) and are linked to a given range of values for each environmental parameter observed within the BGCP. Changes in the distribution of each BGCP (movement, expansion, or contraction) are thereby driven by temporal fluctuations of environmental gradients (i.e., SST, SSS, or [Chl]). Spatial modifications of the location of the BGCPs differ from average seasonal variations quantified in this study (Figure 5 and Table S1). Interestingly, each geographical cell of the Pacific and Indian Oceans was attributed to a given existent BGCP during ENSO period. This result reveals that the environment values during extreme climatic events still ranged into the interval of variation of BGCPs and that no unobserved quadruplet of environmental values exists during this period (e.g., no BGCP attributed). This persistence of BGCPs during ENSO events indicates that the four-dimensional interval of environmental variation defining the environmental envelope could be interpreted as the domain of resilience of each BGCP to climatic variability [*Hughes et al*., 2005] within which BGCPs maintain their environmental characteristics.

[48] The biogeographical methodology proposed in this study belongs to supervised dynamic biogeography as described by the *IOCCG* [2009] (cf. section 1) and uses BGCPs as a geographical reference to model the environmental envelopes using the NPPEN methodology. However, it differs from previous supervised partitions [*Devred et al*., 2007; *Forget et al*., 2010; *Platt et al*., 2005] because we assumed that each province has a characteristic environmental envelope as suggested by *Vichi et al*. [2011]. Here environmental envelopes of each BGCP were characterized using four parameters and deliberately spatially constrained as they aim at approximating the original description that referred to many more ecological parameters. Indeed, several nonquantitative expert knowledge extracted from published ecological and oceanographic studies were used during the identification and in the delineation of BGCPS and their boundaries [*Longhurst*, 2007]. This expert knowledge information (qualitative or expert observations) can thus be hardly quantified by the present statistical methodology.

[49] The visual comparison between our BGCPs and other supervised partitions [*Devred et al*., 2007; *IOCCG*, 2009] shows a global similarity in the spatial distribution and temporal changes of the provinces. Differences with other more objective unsupervised partitions [*IOCCG*, 2009; *Moore et al*., 2002; *Oliver and Irwin*, 2008] can be directly attributed to the environmental or bio-optical parameters chosen to perform the classification or to the difference of methodology. Indeed, the present NPPEN methodology (i.e., probability of occurrence of a given province) is philosophically closer to a fuzzy logic approach [*Moore et al*., 2002] as both approaches rely on the hypothesis that a given geographical cell can belong to different BGCPs [*Matheron*, 1962; *Zadeh*, 1965]. The comparison with the "objective ocean province" proposed by *Oliver and Irwin*

[2008] has revealed a good correspondence despite the higher number of clusters found by the authors. However, these authors were interested in capturing the main mesoscale features (e.g., eddies and current meander) and macroscale features (frontal structure and currents) at a global resolution, whereas our procedure was designed to describe larger spatial features on a wider spatial grid.

[50] Each partition of the ocean that has been proposed in recent decades aimed to delineate the main oceanographical or marine ecological patterns and discontinuities to provide a geographical framework of marine ecosystems or biogeochemical units for ecological studies or management purposes [*IOCCG*, 2009]. In recent years, the increasing amount of observations on both environmental conditions and biological composition of the ocean provided by remote sensing and the constant effort of oceanographic institutes (oceanographic cruises and development of remote or in situ time series) have enabled us to monitor and investigate marine ecosystems at a daily and fine-scale resolution [*Chassot et al*., 2011]. The massive amount of observations available for this study and others [*Oliver and Irwin*, 2008; *Devred et al*., 2007; *Moore et al*., 2002; *Spalding et al*., 2007] has upgraded historical biogeography and provided a more realistic picture of marine ecosystems by refining boundaries and/or by incorporating macroscale/mesoscale ocean dynamics. In this study, we have quantified the environmental envelopes of each BGCP and confirmed their consistency through time and space by quantifying their movements at a seasonal and an interannual time scale. Furthermore, we have identified the distribution of the persistent environmental condition of each province previously quantified by *Vichi et al*. [2011] as well as their seasonal extents and overlaps. In the context of development of ecosystemic approaches for biodiversity and fisheries management and conservation, such modern supervised global distribution of biogeochemical province may be used as a spatial template to monitor, study, and forecast the ecosystem composition and dynamics at each trophic level.

[51] **Acknowledgments.** The authors are grateful to the referees and the Editor who helped to improve the paper. Also, the authors are grateful to S. Bonhommeau, E. Chassot, L. Biermann, F. Benedetti, and P. Koubbi who have improved our understanding on the methodology used in this paper and the interpretation of the results. Also, G.R. and O.M. acknowledge the support of the French ANR, under the grant CEP MACROES (Macroscope for Oceanic Earth System ANR-09-CEP-003). This work is a contribution to the CLIOTOP Synthesis and Modeling Working Group. All outputs of the present paper will be fully available via the website http://www.ecoscopebc.ird.fr/.

## References

Antonov, J. I., R. A. Locarnini, T. P. Boyer, A. V. Mishonov, H. E. Garcia, and S. Levitus (2006), World ocean atlas 2005 vol. 2: Salinity, U.S. Government Printing Office, Washington D.C.

Beaugrand, G., and M. Edwards (2001), Comparison in performance among four indices used to evaluate diversity in pelagic ecosystems, *Oceanol. Acta*, *24*, 467–477.

Beaugrand, G., and P. Helaouët (2008), Simple procedures to assess and compare the ecological niche of species, *Mar. Ecol. Prog. Ser.*, *363*, 29–37.

Beaugrand, G., S. Lenoir, F. Ibañez, and C. Manté (2011), A new model to assess the probability of occurrence of a species, based on presence-only data, *Mar. Ecol. Prog. Ser.*, *424*, 175–190.

Brander, K. (2009), Impacts of climate change on marine ecosystems and fisheries, *J. Mar. Biol. Ass. India*, *51*, 1–13.

Campbell, J. W. (1995), The lognormal distribution as a model for bio-optical variability in the sea, *J. Geophys. Res.*, *100*(C7), 13,237–13,254.

Chassot, E., S. Bonhommeau, G. Reygondeau, K. Nieto, J. J. Polovina, M. Huret, N. K. Dulvy, and H. Demarcq (2011), Satellite remote sensing for an ecosystem approach to fisheries management, *ICES J. Mar. Sci.*, *68*(4), 651–665.

Corbineau, A., T. Rouyer, B. Cazelles, J. M. Fromentin, A. Fonteneau, and F. Ménard (2008), Time series analysis of tuna and swordfish catches and climate variability in the Indian Ocean (1968-2003), *Aquat. Living Resour.*, *21*(3), 277–285.

Cobb, K. M., C. D. Charles, H. Cheng, and R. L. Edwards (2003), El Nino/Southern Oscillation and tropical Pacific climate during the last millennium, *Nature*, *424*, 271–276.

Cullen, J. J., P. J. S. Franks, D. M. Karl, and A. Longhurst (2002), Physical influences on marine ecosystem dynamics, in *The Sea: Biological-Physical Interactions in the Ocean*, vol. *12*, edited by A. R. Robinson, J. J. McCarthy, and B. J. Rothschild, pp. 297–336, John Wiley, New York.

Devred, E., S. Sathyendranath, and T. Platt (2007), Delineation of ecological provinces using ocean colour radiometry, *Mar. Ecol. Prog. Ser.*, *346*, 1–13.

Devred, E., S. Sathyendranath, and T. Platt (2009), Decadal changes in ecological provinces of the NW Atlantic Ocean revealed by satellite observations, *Geophys. Res. Lett.*, *36*, L19607, doi:10.1029/2009GL039896.

Dormann, C. F., J. M. McPherson, M. B. Araújo, R. Bivand, J. Bolliger, G. Carl, R. G. Davies, A. Hirzel, W. Jetz, and W. D. Kissling (2007), Methods to account for spatial autocorrelation in the analysis of species distributional data: A review, *Ecography*, *30*(5), 609–628.

Ducklow, H. W., and R. P. Harris (1993), Introduction to the JGOFS North Atlantic Bloom Experiment, *Deep-Sea Res. II: Top. Stud. Oceanogr.*, *40*, 1–8.

D'Ortenzio, F., and R. M. D'Alcalã (2009), On the trophic regimes of the Mediterranean Sea: A satellite analysis, *Biogeosciences*, *6*, 139–148.

Fonteneau, A. (1998), *Atlas of Tropical Tuna Fisheries,* ORSTOM, Paris.

Forget, M. H., T. Platt, S. Sathyendranath, and P. Fanning (2010), Phytoplankton size structure, distribution, and primary production as the basis for trophic analysis of Caribbean ecosystems, *ICES J. Mar. Sci.*, *68*(4), 751–765.

Goberville, E., G. Beaugrand, B. Sautour, and P. Tréguer (2011), Evaluation of coastal perturbations: A new mathematical procedure to detect changes in the reference state of coastal systems, *Ecol. Indic.*, *11*(5), 1290–1300.

Hardman-Mountford, N. J., T. Hirata, K. A. Richardson, and J. Aiken (2008), An objective methodology for the classification of ecological pattern into biomes and provinces for the pelagic ocean, *Remote Sens. Environ.*, *112*(8), 3341–3352.

Haxeltine, A., and I. C. Prentice (1996), BIOME3: An equilibrium terrestrial biosphere model based on ecophysiological constraints, resource availability, and competition among plant functional types, *Global Biogeochem. Cycles*, *10*(4), 693–709.

Holben, B. N. (1986), Characteristics of maximum-value composite images from temporal AVHRR data, *Int. J. Remote Sens.*, *7*(11), 1417–1434.

Honjo, S., S. J. Manganini, R. A. Krishfield, and R. Francois (2008), Particulate organic carbon fluxes to the ocean interior and factors controlling the biological pump: A synthesis of global sediment trap programs since 1983, *Prog. Oceanogr.*, *76*(3), 217–285.

Hovis, W. A., et al. (1980), Nimbus7 coastal zone color scanner: System description and initial imagery, *Science*, *210*(4465), 60–63.

Hughes, T. P., D. R. Bellwood, C. Folke, R. S. Steneck, and J. Wilson (2005), New paradigms for supporting the resilience of marine ecosystems, *Trends Ecol. Evol.*, *20*, 380–386.

Ibañez, F. (1981), Immediate detection of heterogeneities in continuous multivariate, oceanographic recordings. Application to time series analysis of changes in the bay of Villefranche sur Mer, *Limnol. Oceanogr.*, *26*(2), 336–349.

International Ocean Colour Coordinating Group (IOCCG) (2009), Partition of the ocean into ecological provinces: Role of ocean-colour radiometry, in *Reports and Monographs of the International Ocean-Colour Coordinating Group (IOCCG)*, vol. *9*, edited by M. Dowell, T. Platt, and V. Stuart, pp. 1–98, IOCCG, Dartmouth, Nova Scotia.

Irwin, A. J., and M. J. Oliver (2009), Are ocean deserts getting larger?, *Geophys. Res. Lett.*, *36*, L18609, doi:10.1029/2009GL039883.

Legendre, P., and L. Legendre (1998), *Numerical Ecology*, Elsevier Science, Amsterdam.

Lenoir, S., G. Beaugrand, and E. Lécuyer (2011), Modeled spatial distribution of marine fish and projected modifications in the North Atlantic Ocean, *Global Change Biol.*, *17*(1), 115–129.

Levitus, S. (1982), Climatological atlas of the world ocean, United States Government Printing Office, Washington, D.C.

Longhurst, A. (1995), Seasonal cycles of pelagic production and consumption, *Prog. Oceanogr.*, *36*(2), 77–167.

Longhurst, A. (2007), *Ecological Geography of the Sea*, Academic Press, London.

Mahalanobis, P. C. (1936), On the generalised distance in statistics, *Proc. Nat. Instit. Sci. India*, *2*, 49–55.

Matheron, G. (1962), Traité de géostatistique appliquée, E.B.D.R.G.E. minières, Paris.

McClain, C. R., G. Feldman, and S. Hooker (2004), An overview of the SeaWiFS project and strategies for producing a climate research quality global ocean biooptical time series, *Deep Sea Res., Part II*, *51*, 5–42.

McClain, C. R. (2009), A decade of satellite ocean color observations, *Annu. Rev. Mar. Sci.*, *1*, 19–42.

Messié, M., and F. P. Chavez (2012), A global analysis of ENSO synchrony: The oceans' biological response to physical forcing, *J. Geophys. Res.*, *117*, C09001, doi:10.1029/2012JC007938.

Meyers, G., P. McIntosh, L. Pigot, and M. Pook (2007), The years of El Niño, La Niña, and interactions with the tropical Indian Ocean, *J. Clim.*, *20*, 2872–2880.

Mielke, P. W., K. J. Berry, and G. W. Brier (1981), Application of multi response permutation procedures for examining seasonal changes in monthly mean sea-level pressure patterns, *Mon. Weather Rev.*, *109*, 120–126.

Moore, T. S., J. W. Campbell, and H. Feng (2002), A fuzzy logic classification scheme for selecting and blending satellite ocean color algorithms, *Geosci. Remote Sens.*, *39*(8), 1764–1776.

Oliver, M. J., S. Glenn, J. T. Kohut, A. J. Irwin, O. M. Schofield, M. A. Moline, and, W. P. Bissett (2004), Bioinformatic approaches for objective detection of water masses on continental shelves, *J. Geophys. Res.*, *109*, C07S04, doi:10.1029/2003JC002072.

Oliver, M. J., and A. J. Irwin (2008), Objective global ocean biogeographic provinces, *Geophys. Res. Lett.*, *35*, L15601, doi:10.1029/2008GL034238.

Pauly, D., V. Christensen, R. Froese, A. Longhurst, T. Platt, S. Sathyendranath, K. Sherman, and R. Watson (2000), Mapping fisheries onto marine ecosystems: A proposal for a consensus approach for regional, oceanic and global integrations, paper presented at 88th ICES Annual Science Conference in Session on Classification and Mapping of Marine Habitats, Brugge, Belgium.

Platt, T., H. Bouman, E. Devred, C. Fuentes-Yaco, and S. Sathyendranath (2005), Physical forcing and phytoplankton distributions, *Sci. Mar.*, *69*(Suppl. 1), 55–73.

Platt, T., C. Caverhill, and S. Sathyendranath (1991), Basin-scale estimates of oceanic primary production by remote sensing: The North Atlantic, *J. Geophys. Res.*, *96*(C8), 15,147–15,159.

Platt, T., and S. Sathyendranath (2008), Ecological indicators for the pelagic zone of the ocean from remote sensing, *Remote Sens. Environ.*, *112*(8), 3426–3436.

Polovina, J. J., E. A. Howell, and M. Abecassis (2008), Ocean's least productive waters are expanding, *Geophys. Res. Lett.*, *35* L03618, doi:10.1029/2007GL031745.

Radenac, M.-H., F. Léger, A. Singh, and T. Delcroix (2012), Sea surface chlorophyll signature in the tropical Pacific during eastern and central Pacific ENSO events, *J. Geophys. Res.*, *117*, C04007, doi:10.1029/2011JC007841.

Reygondeau, G., and G. Beaugrand (2011), Water column stability and *Calanus finmarchicus*, *J. Plankt. Res.*, *33*(1), 119–136.

Reygondeau, G., O. Maury, A. Fonteneau, J. M. Fromentin, G. Beaugrand, and P. Cury (2012), Biogeography of tuna and billfish communities, *J. Biogeogr.*, *39*, 114–129.

Rouyer, T., J. M. Fromentin, N. C. Stenseth, and B. Cazelles (2008), Analysing multiple time series and extending significance testing in wavelet analysis, *Mar. Ecol. Prog. Ser.*, *359*, 11–23.

Rosa, H. Jr., and T. Laevastu (1960), Comparison of biological and ecological characteristics of sardines and related species—A preliminary study, in *Proc. World Scientific Meeting on the Biology of Sardines and Related Species*, edited by H. Rosa and G. Murphy, p. 523-552, Rome, Italy.

Sarmiento, J. L., and N. Gruber (2006), *Ocean Biogeochemical Dynamics*, Princeton University Press, Princeton, N. J.

Sathyendranath, S., A. Longhurst, C. M. Caverhill, and T. Platt (1995), Regionally and seasonally differentiated primary production in the North Atlantic, *Deep-Sea Res. I: Oceanogr. Res. Pap.*, *42*(10), 1773–1802.

Scientific Committee on Oceanic Research (1990), The Joint Global Ocean Flux Study science plan, JGOFS rep. 5, pp. 61, Halifax, Canada.

Sherman, K. (2005), The large marine ecosystem approach for assessment and management of ocean coastal waters, in *Sustaining Large Marine Ecosystems: The Human Dimension*, edited by T. M. Hennessey and J. G. Sutinen, pp. 3–16, Elsevier B.V., Amsterdam, The Netherlands.

Smith, W. H. F., and D. T. Sandwell (1997), Global sea floor topography from satellite altimetry and ship depth soundings, *Science*, *277*, 1956–1962.

Spalding, M. D., et al. (2007), Marine ecoregions of the world: A bioregionalization of coastal and shelf areas, *BioScience*, *57*(7), 573–583.

Schwing, F. B., T. Murphree, and P. M. Green (2002), The Northern Oscillation Index (NOI): A new climate index for the northeast Pacific, *Prog. Oceanogr.*, *53*, 115–139.

Sverdrup, H. U. (1953), On conditions for the vernal blooming of phytoplankton, *ICES J. Mar. Sci.*, *18*, 287–295.

Tomczak, M., and J. S. Godfrey (2003), *Regional Oceanography: An Introduction*, Daya Publishing House, Delhi, India.

Vichi, M., J. I. Allen, S. Masina, and N. J. Hardman-Mountford (2011), The emergence of ocean biogeochemical provinces: A quantitative assessment and a diagnostic for model evaluation. *Global Biogeochem. Cycles*, *25*, GB2005, doi:10.1029/2010GB003867.

Vantrepotte, V., and F. Mélin (2010), Temporal variability in SeaWiFS derived apparent optical properties in European seas, *Cont. Shelf Res.*, *30*, 319–334.

Whittaker, R. H. (1975), *Communities and Ecosystems*, Macmillan, New York.

Zadeh, L. A. (1965), Fuzzy sets, *Inf. Control*, *8*(3), 338–353.